CrossMark

Generation and wired/wireless transmission of IEEE802.16m signal using solitons generated by microring resonator

**S. E. Alavi · I. S. Amiri ·
S. M. Idrus · A. S. M. Supa'at**

© Springer Science+Business Media New York 2014

Abstract Multi-carrier generation is the main building block for generating WiMax signal. In order to use WiMax signal in radio over fiber applications the use of all optical generation of RF signals is required. To generate multi carriers optically, the system consisting of series of microring resonators (MRRs) incorporating with an add/drop filter system are used. Thus the high frequency (THz) solitons range of 193.29–193.35 THz at frequencies of 193.333, 193.3355 and 193.3388 THz with the free spectral range of 2.5 and 5.8 GHz could be performed using MRRs, providing required WiMax signal used in wired/wireless communication. The generated multi carriers are multiplexed with the single carrier soliton and transmitted through single mode fiber (SMF) after being beaten to photodiode, a WiMax signal is propagated wirelessly in transmitter antenna base station and is received by the second antenna located in the receiver. Here, based on the switching of channel 1 or channel 2, the 2.5 or 5.8 GHz RF WiMax can be generated. When the RF signal is up-converted at the receiver central office, the detected signal is analysed in order to evaluate the error vector magnitude (EVM) of each wireless channel. As results, both channels show a soft EVM variation for different path lengths, where the transmission of both channels is feasible for up to a 50 km SMF path length.

Keywords WiMax signal · OFDMA · Multi-carrier · High frequency (THz) ·
IEEE802.16m

1 Introduction

In recent years a growth in demand for wireless network technologies motivated the development of a new network technology standard (Chang et al. 2012). Since January 2007 IEEE workgroup has been developing IEEE 802.16 standard which in turn developed into the IEEE

S. E. Alavi · I. S. Amiri (✉) · S. M. Idrus · A. S. M. Supa'at
Lightwave Communication Research Group, Faculty of Electrical Engineering,
Universiti Teknologi Malaysia (UTM), 81310 Skudai, Johor, Malaysia
e-mail: isafiz@yahoo.com

802.16m standard or broadband wireless access (BWA) better known as worldwide interoperability for microwave access (WiMAX) (Nafea et al. 2013). IEEE 802.16m amends the IEEE 802.16e wireless metropolitan area network standard to meet the cellular layer requirements of the International Telecommunication Union–Radio communication International Mobile Telecommunications–advanced next generation mobile networks (4G systems) (So-In et al. 2009). The WiMAX air interface promises high bandwidth rates, capable of data transfer rates up to 1Gb/s depending on the available bandwidth and multiple antenna mode, which can cover metropolitan area of several kilometers (Group 2004). In theory, a WiMAX can cover an area of 35 miles (56 kms) for fixed stations and 3–10 miles (5–15 kms) for mobile stations (MSs). The foreseen backward compatibility of IEEE 802.16m standard enables the smooth evolution of current WiMAX systems and easy deployment with the legacy MSs and base stations. While the technology mostly is primarily focused on IP-based services, it also supports Ethernet as it is an important factor for some fixed access deployments (Srikanth et al. 2012).

WiMAX air interface includes the medium access control and physical (PHY) layers of BWA in which multiple accesses is achieved through orthogonal frequency-division multiplexing access (OFDMA) in the PHY layer of the air interface that assigns a subset of subcarriers to each individual user (Carro-Lagoa et al. 2013; Kanonakis et al. 2012). OFDM enables downlink and uplink multi-input multi-output (MIMO) as well as beam forming (BF) features. Furthermore, IEEE 802.16m uses multi-hop relay architectures for improved coverage and performance (Chuang et al. 2012). The WiMAX is similar to the wireless standard known as Wi-Fi, but on a much larger scale and at faster speeds. A nomadic version would keep WiMAX-enabled devices connected over large areas, much like today's cell phones. A single WiMAX antenna is expected to have a range of up to 40 miles with 5 bps/Hz spectral efficiency and its speed can goes up to 100 Mbps in a Flexible channel sizes from 1.5 to 20 MHz. As such, WiMAX can bring the underlying Internet connection needed to service local Wi-Fi networks from one to hundreds of Consumer Premises Equipments (CPE)s, with unlimited subscribers behind each CPE (Tsolkas et al. 2012). WiMax will provide your several levels of quality of service and provides ubiquitous broadband.

Multi-carrier generation is the main building block for generating WiMax signal. In order to use WiMax signal in radio over fiber applications the use of all optical generation of RF signals can help to reduce the challenges of electronic devices. One solution to generate multi carriers optically is to use the microring resonator (MRR) systems (Amiri et al. 2013). Nonlinear light behaviour inside an MRR occurs when a strong pulse of light is inputted into the ring system, which is used in many applications in signal processing and communication (Spyropoulou et al. 2011). The properties of a ring system can be modified via various control methods. Ring resonators can be used as filter devices where generation of high frequency (THz) soliton signals can be performed using suitable system parameters (Lin and Crozier 2011). The series of MRRs connected to an add/drop filter system, is used in many applications in optical communication and signal processing. This system can be used to generate optical soliton pulses of THz frequencies, thus providing required signals used in wired/wireless optical communication such as all optical OFDM to be applied for WiMax applications.

In this study, series of ring resonators are connected to an add/drop system in order to generate multi-carriers which are applied to implement the optical OFDM suitable for the WiMax communication systems. Results show that MRR systems support both single and multi-carrier optical soliton pulses that are used in an OFDM transmitter/receiver system. Here, the optical soliton in a nonlinear fiber MRR system is analyzed in order to generate a high frequency band (THz) of pulses as single and multi-carrier signals where multi-carriers
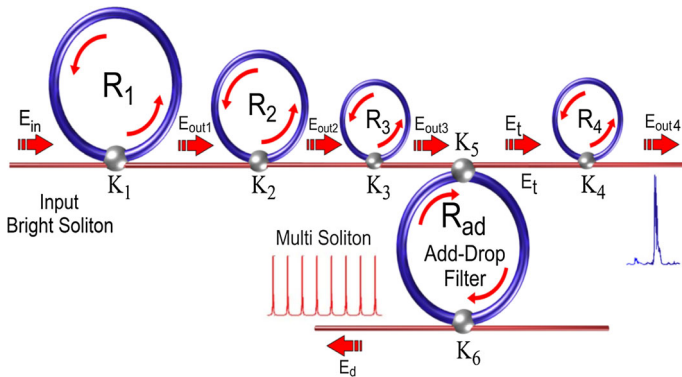
Fig. 1 MRR system—R: ring radii, κ: coupling coefficients, R_{ad}: add/drop ring radius, E_{in}: input power, E_{out}: Ring resonator output E_t: throughput output, E_d: drop port output

are used for generating one optical WiMax channel band. The generated signal is multiplexed with a single carrier soliton and transmitted through single mode fiber (SMF) after being beaten to photodiode an IEEE802.16m signal is propagated wirelessly in transmitter antenna base station and is received by the second antenna located in the receiver. The bit error rate and error vector magnitude (EVM) of the overall system are also discussed.

2 Theoretical background

The system of THz frequency band generation is shown in Fig. 1. Here, a series of MRRs are used incorporating to an add/drop filter system. The filtering process of the input soliton pulses is performed via the MRRs, where frequency band ranges of 193.29–193.35 THz can be obtained. A large output gain is obtained by the soliton self-phase modulation that is required to balance the dispersion effects of the linear medium. This system is shown in Fig. 1.

Ring resonators are made of fiber optics where the medium has Kerr effect-type nonlinearity. The Kerr effect causes the refractive index (n) of the medium to vary; it is given by

$$n = n_0 + n_2 I = n_0 + \frac{n_2}{A_{eff}} P, \tag{1}$$

where n_0 and n_2 are the linear and nonlinear refractive indices, respectively, and I and P are the optical intensity and the power, respectively. The effective mode core area given by A_{eff} ranges from 0.10 to 0.50 μm^2 in terms of material parameters (InGaAsP/InP). A bright soliton with a central frequency of 1.55 μm and power of 800 mW is introduced into the first ring resonator, R_1 expressed by E_{in}. The input optical field of the optical bright soliton is given by

$$E_{in} = A \sec h \left[\frac{T}{T_0} \right] \exp \left[\left(\frac{z}{2L_D} \right) - i\omega_0 t \right], \tag{2}$$

where A and z are the amplitude of the optical field and propagation distance, respectively, L_D is the dispersion length of the soliton pulse, and the carrier frequency of the signal is ω_0. The soliton pulse keeps its temporal width invariance while it propagates; therefore, it

is called a temporal soliton. A balance should be achieved between the dispersion length (L_D) and the nonlinear length ($L_{NL} = 1/\Gamma\phi_{NL}$). Here, $\Gamma = n_2 \times k_0$ is the length scale over which disperse or nonlinear effects make the beam become wider or narrower; hence, $L_D = L_{NL}$. The normalized output of the light field, which is the ratio between the output and the input fields for each round trip, can be expressed by:

$$\left| \frac{E_{out1,out2,out3}(t)}{E_{in,out1,out2}(t)} \right|^2$$

$$= (1-\gamma) \left[1 - \frac{\left(1 - (1-\gamma)x_{1,2,3}^2 \right) \kappa_{1,2,3}}{(1 - x_{1,2,3}\sqrt{1-\gamma}\sqrt{1-\kappa_{1,2,3}})^2 + 4x_{1,2,3}\sqrt{1-\gamma}\sqrt{1-\kappa_{1,2,3}}\sin^2\left(\frac{\phi_{1,2,3}}{2}\right)} \right]$$

$$(3)$$

κ is the coupling coefficient, and $x = exp(-\alpha L/2)$ represents the round trip loss coefficient, where the ring resonator length and linear absorption coefficient are given by L and α, respectively. $\phi = \phi_0 + \phi_{NL}$, where $\phi_0 = kLn_0$ and $\phi_{NL} = kLn_2|E_{in}|^2$ are the linear and nonlinear phase shifts, respectively (Amiri and Ali 2013). The wave propagation number in vacuum and the fractional coupler intensity loss are given by $k = 2\pi/\lambda$ and γ, respectively. The bright soliton pulse is input into the nonlinear MRRs. By applying the appropriate parameters, a chaotic signal can be formed. For the add/drop system, the interior electric fields (E_a and E_b) are expressed as

$$E_a = \frac{E_{out3} \times j\sqrt{\kappa_5}}{1 - \sqrt{1-\kappa_5}\sqrt{1-\kappa_6}e^{\frac{-\alpha}{2}L_{ad} - jk_n L_{ad}}}$$

$$(4)$$

$$E_b = \frac{E_{out3} \times j\sqrt{\kappa_5}}{1 - \sqrt{1-\kappa_5}\sqrt{1-\kappa_6}e^{\frac{-\alpha}{2}L_{ad} - jk_n L_{ad}}} \cdot \sqrt{1-\kappa_6}e^{\frac{-\alpha}{2}\frac{L_{ad}}{2} - jk_n \frac{L_{ad}}{2}}$$

$$(5)$$

where κ_5 and κ_6 are the coupling coefficients, $L_{ad} = 2\pi R_{ad}$, and R_{ad} is the radius of the add/drop system. The throughput and drop port electrical fields of the add/drop system can be expressed as

$$E_t = E_b e^{\frac{-\alpha}{2}\frac{L_{ad}}{2} - jk_n \frac{L_{ad}}{2}}j\sqrt{\kappa_5} + E_{out3} \times \sqrt{1-\kappa_5}$$

$$(6)$$

$$E_d = E_a e^{\frac{-\alpha}{2}\frac{L_{ad}}{2} - jk_n \frac{L_{ad}}{2}}j\sqrt{\kappa_6}$$

$$(7)$$

Thus,

$$\frac{E_t}{E_{out3}} = \frac{-\kappa_5\sqrt{1-\kappa_6}e^{\frac{-\alpha}{2}L_{ad} - jk_n L_{ad}} + \sqrt{1-\kappa_5} - (1-\kappa_5)\sqrt{1-\kappa_6}e^{\frac{-\alpha}{2}L_{ad} - jk_n L_{ad}}}{1 - \sqrt{1-\kappa_5}\sqrt{1-\kappa_6}e^{\frac{-\alpha}{2}L_{ad} - jk_n L_{ad}}}$$

$$= \frac{-\sqrt{1-\kappa_6}e^{\frac{-\alpha}{2}L_{ad} - jk_n L_{ad}} + \sqrt{1-\kappa_5}}{1 - \sqrt{1-\kappa_5}\sqrt{1-\kappa_6}e^{\frac{-\alpha}{2}L_{ad} - jk_n L_{ad}}}$$

$$(8)$$

$$\frac{E_d}{E_{out3}} = \frac{-\sqrt{\kappa_5.\kappa_6}e^{\frac{-\alpha}{2}\frac{L_{ad}}{2} - jk_n \frac{L_{ad}}{2}}}{1 - \sqrt{1-\kappa_5}\sqrt{1-\kappa_6}e^{\frac{-\alpha}{2}L_{ad} - jk_n L_{ad}}}$$

$$(9)$$

The normalized optical outputs of the ring resonator add/drop system can be expressed by Eqs. (10) and (11):

$$\frac{|E_t|^2}{|E_{out3}|^2} = \frac{(1 - \kappa_5) - 2\sqrt{1 - \kappa_5} \cdot \sqrt{1 - \kappa_6}e^{-\frac{\alpha}{2}L_{ad}}\cos(k_nL_{ad}) + (1 - \kappa_6)e^{-\alpha L_{ad}}}{1 + (1 - \kappa_5)(1 - \kappa_6)e^{-\alpha L_{ad}} - 2\sqrt{1 - \kappa_5} \cdot \sqrt{1 - \kappa_6}e^{-\frac{\alpha}{2}L_{ad}}\cos(k_nL_{ad})} \tag{10}$$

$$\frac{|E_d|^2}{|E_{out3}|^2} = \frac{\kappa_5\kappa_6 e^{-\frac{\alpha}{2}L_{ad}}}{1 + (1 - \kappa_5)(1 - \kappa_6)e^{-\alpha L_{ad}} - 2\sqrt{1 - \kappa_5} \cdot \sqrt{1 - \kappa_6}e^{-\frac{\alpha}{2}L_{ad}}\cos(k_nL_{ad})} \tag{11}$$

where $|E_t|^2$ and $|E_d|^2$ are the optical output powers of the through and drop ports, respectively, whereas the output electric field from the third ring is given by E_{out3}. The nonlinear refractive index can be neglected for the add/drop system. The throughput output from the add/drop system enter the forth ring resonator where the filtering of the signals leads to generate ultra-short THz solitons. Here the output signal of the forth ring resonator is expressed by E_{out4}, where

$$\left|\frac{E_{out4}(t)}{E_t(t)}\right|^2$$

$$= (1 - \gamma)\left[1 - \frac{(1 - (1 - \gamma)x_4{}^2)\kappa_4}{1 - x_4\sqrt{1 - \gamma}\sqrt{1 - \kappa_4}^2 + 4x_4\sqrt{1 - \gamma}\sqrt{1 - \kappa_4}\sin^2\left(\frac{\phi}{2}\right)}\right] \tag{12}$$

3 Results of soliton generation

The fixed and variable parameters of the MRR system are listed in Table 1.

The results of the chaotic signal generation are shown in Fig. 2. The input pulse of the bright soliton pulse with a power of 800 mW is inserted into the system. Large bandwidth within the MRRs can be generated by using a bright soliton pulse input into the nonlinear system. The signal is chopped (sliced) into smaller signals spreading over the spectrum; thus, a large bandwidth is formed by the nonlinear effects of the medium. A frequency soliton pulse can be formed and trapped within the system with suitable ring parameters. The chaotic soliton pulses are used widely as carrier signals in securing optical communication, wherein the information is input into the signals and ultimately can be retrieved by using suitable filtering systems. Filtering of the soliton signals can be performed when the pulses pass through the MRRs. The output signals from the system can be seen in Fig. 2, where soliton pulses ranges of 193.29–193.35 THz are generated and used in WiMax communication, wireless personal area networks and wireless local area networks. The forth MRR's output [$E_{out4}(t)$] shows localized ultra-short soliton pulses with free spectral range (FSR) of 2.5 and 5.8 GHz, where soliton pulses at frequencies of 193.333, 193.3355 and 193.3388 GHz are generated. The drop port output expressed by E_d is shown in Fig. 2g, h, where multi-soliton pulses with FSR of 6.66 MHz could be generated. For doing so the band pass filter is used to pick out the four carriers shown in Fig. 2h.

Table 1 Fixed and variable parameters of the MRR system

Fixed parameters	Variable parameters
$R_{Add/Drop} = 550\,\mu m$	$T_0 = $ Initial propagation time
$R_1 = 15\,\mu m$	$T = $ Propagation time
$R_2 = 9\,\mu m$	$z = $ Propagation distance
$R_3 = 6\,\mu m$	$L_D = $ Dispersion length
$R_4 = 6\,\mu m$	$L_{NL} = $ Nonlinear length
$\kappa_1 = 0.98$	$\phi = $ Total phase shift
$\kappa_2 = 0.98$	$\phi_{NL} = $ Nonlinear phase shift
$\kappa_3 = 0.96$	$\phi_0 = $ Linear phase shift
$\kappa_4 = 0.92$	$A = $ Optical amplitude
$\kappa_5 = 0.05$	$I = $ Optical intensity
$\kappa_6 = 0.05$	$P = $ Optical power
$n_0 = 3.34$	$E_1, E_2 = $ Interior electric fields
$n_2 = 2.4 \times 10^{-17} m^2 W^{-1}$	$E_{out} = $ Electric field of the ring resonator
$A_{eff1} = 0.50\,\mu m^2$	$E_t = $ Throughput electric field
$A_{eff2} = 0.25\,\mu m^2$	$E_d = $ Drop port electric field
$A_{eff3} = 0.10\,\mu m^2$	
$\alpha = 0.5\,dB\,mm^{-1}$	
$\gamma = 0.1$	
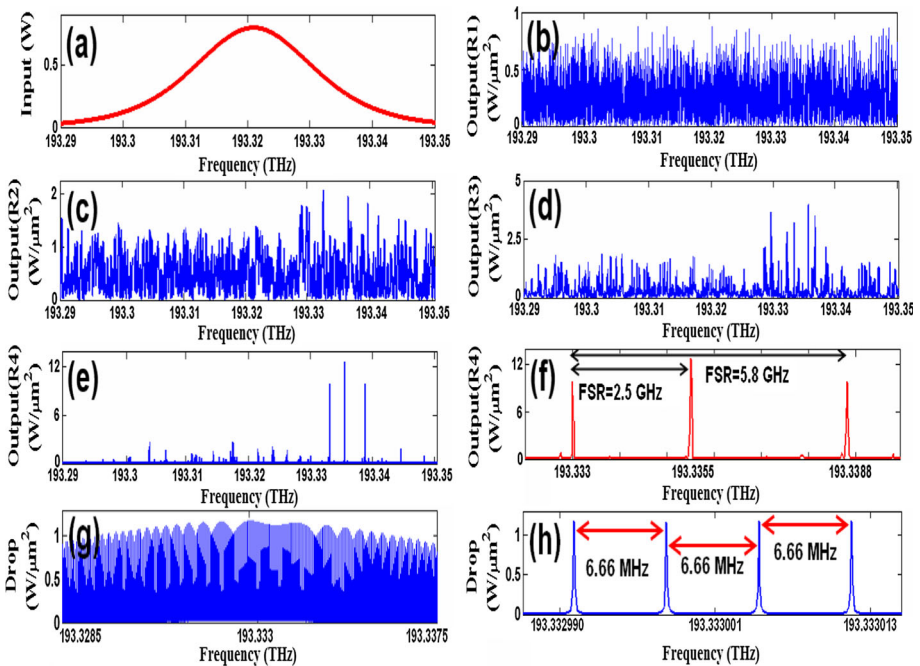
Fig. 2 Results single and multi-carriers: **a** Input bright soliton, **b** output from first ring, **c** output from second ring, **d** output from third ring, **e** output from the fourth ring, **f** expansion of the output R_4, **g** drop port output, **h** expansion of the output E_d
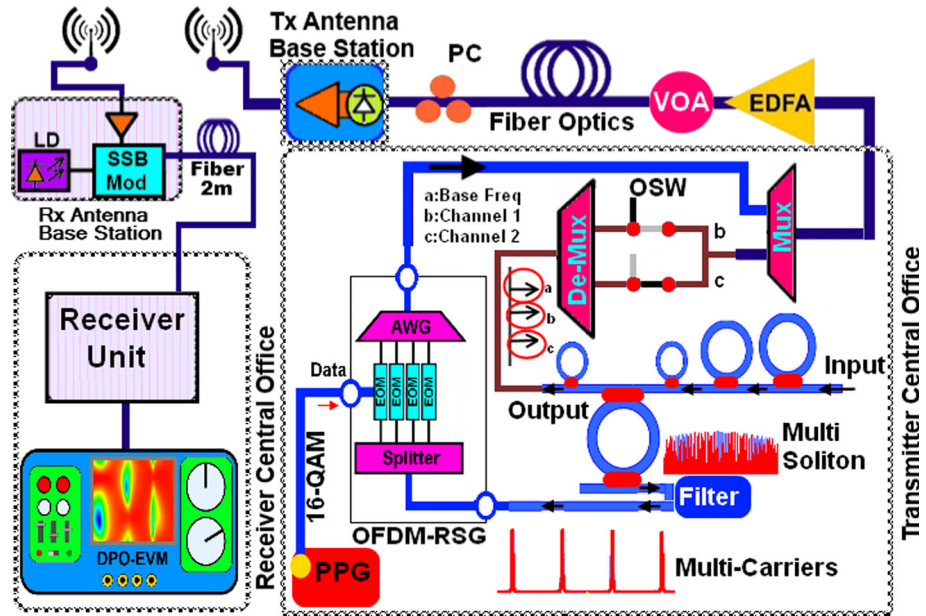
**Fig. 3** System setup

4 System setup

The schematic of the system setup is shown in Fig. 3. At the transmitter central office (TCO) a series of MRRs are connected to an add/drop system in order to generate single and multi soliton carriers as discussed in previous section.

4.1 WiMax signal generation

In this stage the WiMax signal is generated optically by using the OFDM signal generator module (OFDM-SGM). This module has one optical and one electrical input and one optical output port. The electrical input port is connected to the pulse pattern generator which generates 16-QAM data signal. Optical input is the multi-carriers centered shown in Fig. 2h. In order to generate all optical OFDM signal, multi-carriers are first separated by the optical splitter then, they are modulated via16-QAM signal from the PGG using external optical modulator. Afterwards, in order to characterize the IFFT block at the transmitter an array waveguide grating is used (Wang et al. 2011).

The spectra of the modulated optical subcarriers are overlapped which form one optical OFDM channel band. Then the generated all optical OFDM signal is multiplexed by the wavelength located at b:193.3355 or c:193.3388 i.e. channel 1 and channel 2. The distance between the center of OFDM signal and the center of the single carriers is (a–b) 2.5 GHz or (a–c) 5.8 GHz which are the RF band for WiMax standard.

These two channels are separated with de-multiplexer and using optical switch, one of them is switched into multiplexer with the base carrier (a) and after amplification by an erbium doped fiber amplifier the multiplexed signal is transmitted through the SMF. The nonlinear refractive index is 2.6×10^{-20} m^2/W, where the fiber optic has a length of L=10, 25, and 50 km, attenuation of 0.2 dB/km, dispersion of 5 ps/nm/km, the differen-
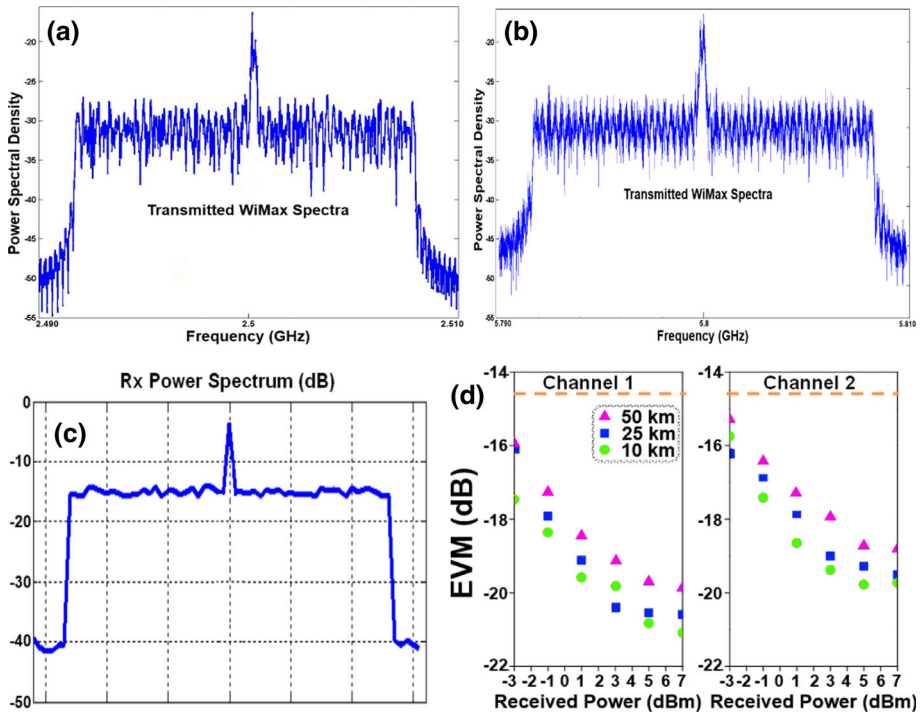
Fig. 4 Transmitter and receiver performance

tial group delay of 0.2 ps/km, effective area of $25\,\mu m^2$ and the nonlinear phase shift of 3 mrad.

In order to investigate the optical link performance, the total optical power level after amplification is adjusted with a variable optical attenuator from -3 to 7 dBm. The joint signal is received at the transmitter antenna base station and in order to maximize the photoreceiver performance, the state of the polarization can be adjusted by a polarization controller. The multiplexed signals are being beaten to a PIN photodetector (0.7 A/W responsivity) therefore a RF WiMax signal is generated and propagated wirelessly by the transmitter antenna. Here, based on the switching of channel 1 or channel 2, whether 2.5 or 5.8 GHz RF WiMax are generated and are shown in Fig. 4a, b respectively.

At the receiver antenna base station, the propagated RF WiMax is received which is shown in Fig. 4c. Here the RF signal is up-converted using a commercially available distributed feedback laser to process the received signal optically. Now the up-converted signal is transmitted to receiver central office (RCO) through 2 m SMF. At the RCO the detected signal is amplified and analyzed in order to evaluate the EVM of each wireless channel. EVM measurement as a figure of merit for assessing the quality of digital communication signals is performed to evaluate the link degradation.

The EVM results for channels 1 and 2 at different optical power and in different optical path lengths are shown in Fig. 4d. The -14.5 dB EVM is the threshold for successful transmission which is shown with a dashed line. As it is clear in results for different optical power both channels show a soft EVM variation for different path lengths. Therefore it could be concluded that the transmission of both channels is feasible for up to a 50 km SMF path length. A further investigation on system performance is conducted using a bit error rate calculation.
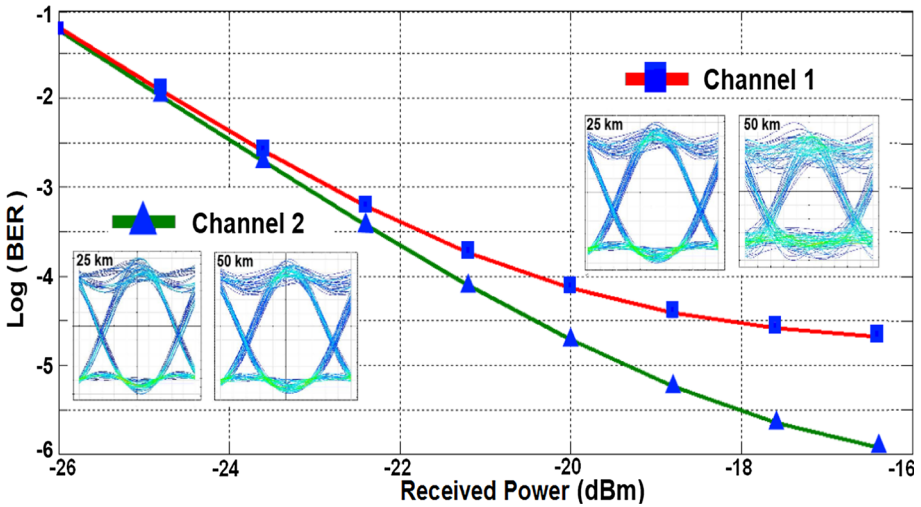
Fig. 5 The system performance under two channel 1 and channel 2

As illustrated in Fig. 5, the system performance under two circumstances is investigated which are channel 1 and channel 2. As can be concluded from this figure by increasing the received power, channel 2 outperforms the other one.

Based on the presented system and results it is possible to use MRR to generate both single and multi-carriers which can be applied to the optical generation of WiMax signal. IEEE802.16e is a common application which can be benefited from this system.

5 Conclusion

A series of MRRs incorporating with an add/drop filter system are used to generate THz frequency band. The filtering of the input pulse within the system causes the generation of single and multi soliton pulses used in WiMax communication. THz solitons range of 193.29–193.35 THz at frequencies of 193.333, 193.3355 and 193.3388 THz with the FSR of 2.5 and 5.8 GHz was achieved using MRRs, providing required WiMax signals used in wired/wireless communication. All optically generated WiMax signal was used in radio over fiber applications. Results clarified that two WiMax channels with 2.5 and 5.8 GHz central frequencies have a soft EVM variation for different path lengths; therefore the transmission of both channels is feasible for up to a 50 km SMF path length.

References

Amiri, I.S., Ali, J.: Data signal processing via a manchester coding-decoding method using chaotic signals generated by a PANDA ring resonator. Chin. Opt. Lett. **11**(4), 041901–041904 (2013)

Amiri, I.S., Soltanmohammadi, S., Shahidinejad, A., Ali, J.: Optical quantum transmitter with finesse of 30 at 800-nm central wavelength using microring resonators. Opt. Quantum Electron. **45**(10), 1095–1105 (2013)

Carro-Lagoa, Á., Suárez-Casal, P., García-Naya, J.A., Fraga-Lamas, P., Castedo, L., Morales-Méndez, A.: Design and implementation of an OFDMA-TDD physical layer for WiMAX applications. EURASIP J. Wirel. Commun. Netw. **2013**(1), 1–19 (2013)

Chang, K., Deb, S., Ganguly, A., Yu, X., Sah, S.P., Pande, P.P., Belzer, B., Heo, D.: Performance evaluation and design trade-offs for wireless network-on-chip architectures. ACM J. Emerg. Technol. Comput. Syst. (JETC) **8**(3), 1–23 (2012)

Chuang, Y., Tseng, H., Sheu, S.: A performance study of discrete-error-checking scheme (DECS) with the optimal division locations for IEEE 802.16-based multi-hop networks. IEEE Trans. Comput. **62**(12), 2354–2365 (2012)

Group, I. W.: IEEE standard for local and metropolitan area networks, Part 16: air interface for fixed broadband wireless access systems. IEEE Std. **802**, 16 (2004)

Kanonakis, K., Tomkos, I., Krimmel, H., Schaich, F., Lange, C., Weis, E., Leuthold, J., Winter, M., Romero, S., Kourtessis, P., Milosavljevic, M., Cano, I.N., Prat, O.: An OFDMA-based optical access network architecture exhibiting ultra-high capacity and wireline-wireless convergence. Commun Mag IEEE, **50**(8), 71–78 (2012)

Lin, S., Crozier, K.B.: Planar silicon microrings as wavelength-multiplexed optical traps for storing and sensing particles. Lab Chip **11**(23), 4047–4051 (2011)

Nafea, H.B., Zaki, F.W., Moustafa, H.E.: Performance and capacity evaluation for mobile WiMAX IEEE 802.16m standard. Nature **1**(1), 12–19 (2013)

So-In, C., Jain, R., Tamimi, A.-K.: Scheduling in IEEE 802.16e mobile WiMAX networks: key issues and a survey. IEEE J. Sel. Areas Commun. **27**(2), 156–171 (2009)

Spyropoulou, M., Pleros, N., Miliou, A.: SOA-MZI-based nonlinear optical signal processing: a frequency domain transfer function for wavelength conversion, clock recovery, and packet envelope detection. IEEE J. Quantum Electron. **47**(1), 40–49 (2011)

Srikanth, S., Pandian, M., Fernando, X.: Orthogonal frequency division multiple access in WiMAX and LTE: a comparison. IEEE Commun. Mag. **50**(9), 153–161 (2012)

Tsolkas, D., Xenakis, D., Passas, N., Merakos, L.: Next generation cognitive cellular networks, LTE, WiMAX and wireless broadband access. In: Hrishikesh V., Gabriel-Miro M (eds.) Cognitive Radio and its Application for Next Generation Cellular and Wireless Networks. pp. 307–330. Springer, Berlin (2012)

Wang, Z., Kravtsov, K.S., Huang, Y.-K., Prucnal, P.R.: Optical FFT/IFFT circuit realization using arrayed waveguide gratings and the applications in all-optical OFDM system. Opt. Express **19**(5), 4501–4512 (2011)